QUANTITATIVE POROSITY MAPPING OF RESERVOIR ROCK CORES BY PHYSICALLY SLICE SELECTED NMR

Alun J. Lucas, Greg K. Pierens, Mark Peyron, T. Adrian Carpenter, Laurance D. Hall, Robert C. Stewart*, Daniel W. Phelps*, Gary F. Potter*
Herchel Smith Laboratory for Medicinal Chemistry
University Forvie Site, Robinson Way
Cambridge, CB2 2PZ, UK
* Amoco Production Company
Tulsa Research Centre, 4502 East 41st Street
P.O. Box 3385, Tulsa, Oklahoma 74102, USA

Abstract A unique feature of NMR saturation measurements is the facility to study the saturation state in a defined region of a long (≥1 foot) core sample and thus measure the porosity profile. This paper addresses the three steps necessary to implement quantitative physical slice selection: (i) construction of a NMR probe of dimensions commensurate with the slice thickness required, (ii) demonstration that the characteristics of the probe are appropriate for quantitative porosity measurements and (iii) establishing and testing a NMR measurement protocol.

The results reported were obtained with a Bruker MSL300 console in conjunction with a Bruker 2 kW class C amplifer and an Oxford Instruments 31 cm horizontal bore superconducting magnet operating at 0.66 T (28.3 MHz for ^{1}H NMR).

The dimensions of the physical slice are primarily controlled by the size of the NMR probe and the position of radiofrequency screening. Two options can be considered to define a physical slice; first, the slice thickness can be determined solely by the length of the NMR probe, and second, radiofrequency screening can be implemented to modify the slice profile from a

longer length probe. Both approaches have been evaluated, the first in detail.

This method has been developed into a practical system and used to measure the axial porosity profiles of three brine saturated long core samples: Berea sandstone, Bedford limestone and a composite core sample. For the Berea core a mean NMR porosity of 13.0±0.3% was obtained; the gravimetric porosity was 13.4±0.1%. The corresponding values for the Bedford core are 13.8±0.3 and 13.3±0.1% porosity, respectively. Both of these samples exhibit homogeneous porosity distributions.

To investigate heterogeneous porosity distributions a composite of five short cores, including both sandstones and carbonates, was studied. The NMR porosity profile obtained clearly maps the porosity variation, based on the individual core porosities, and integration of the profile gave a mean porosity of 19.8±0.6% ; the gravimetric porosity was calculated similarly giving 20.8±0.1%.

INTRODUCTION

The utility of nuclear magnetic resonance (NMR) techniques in petrophysical applications has been demonstrated in a number of publications to date. Core analysis applications range from the direct determination of saturations (Edelstein *et al.*, 1988; Osment *et al.*, 1990) to the study of pore geometry via NMR diffusion (Mitra and Sen, 1992) and connectivity via NMR flow measurements (Woessner *et al.*, 1990; Guilfoyle *et al.*, 1992). Recent publications which present quantitative porosity and saturation measurements have demonstrated the feasibility of routine, automated analysis (Vinegar *et al.*, 1989; Edelstein *et al.*, 1990). As this range of applications, both spectroscopy and imaging, expands it is apparent that before NMR methods attain widespread acceptance and use within the oil industry it is necessary to demonstrate the accuracy and precision of the resulting data.

To assess the level of quantitation attainable under complex experimental conditions (*e.g.*, two phase displacement processes) we have undertaken a series of experiments designed to determine the accuracy and precision of each component of the experiment. The first experiment was to demonstrate quantitative NMR measurements of brine saturations in single-phase brine-saturated rock cores which were small enough to fit completely within a NMR probe. We have developed a single, robust NMR protocol for those measurements and extended the range of core

samples studied in order to determine the accuracy and precision attainable in routine use. Using this protocol the brine content of a variety of reservoir rock cores is measured with a mean absolute error of 0.3% porosity (Lucas *et al.*,). The next step extends this NMR protocol to quantitative NMR measurements of oil and brine saturations in mixed-phase saturated cores and incorporates quantitative NMR slice selection.

Quantitative NMR slice selection is important for two main reasons. First, NMR measurements of the mixed phase saturations of rock core samples extracted during exploratory drilling involves measuring long core samples which extend beyond the limits of a NMR probe. This makes quantitative NMR measurements difficult for three reasons: (i) inhomogeneities in the static magnetic field, B_0, applied to the core sample, (ii) spatial variations in the amplitude of the time-dependent magnetic field, B_1, applied to perturb the nuclear spin system from equilibrium and (iii) probe loading effects produced by the conducting core sample. A second reason for interest in NMR slice selection is associated with NMR imaging applications. Slice selection in NMR imaging involves the application of a magnetic field gradient allied with a frequency selective excitation pulse; by definition such pulses are generally of relatively long duration (>0.5 ms). However, for quantitative measurements it is important that the duration of any excitation pulse be short compared with the duration of the time domain NMR signal from the pore fluid. In practice the latter is short due to the rapid dephasing of magnetization in rock core systems arising from magnetic susceptibility differences between the rock matrix and pore fluid.

Two approaches are available for studying localized volumes within a core; (i) physical slice selection incorporating slice selection controlled solely by the dimensions of the NMR probe and any associated radiofrequency screening and (ii) radiofrequency NMR slice selection by any method utilizing a frequency selective excitation pulse. In this study single-phase brine-saturated cores are studied via physical slice selection methods, which is particularly important for quantitative saturation measurements on long core samples which exhibit rapid time domain NMR signal decay. To our knowledge this is the first publication to specifically address the question of quantitative physical NMR slice selection methods for core analysis applications.

Existing conventional techniques for determining core sample porosity and saturations establish the accuracy criteria for comparable NMR core analysis; for example, the maximum acceptable deviation in a standard core plug porosity

measurement using a Boyle's Law apparatus is 0.5% porosity (Thomas and Pugh, 1989).

The basic principles and terminology of NMR (Lauterbur, 1973; Sanders and Hunter, 1987) are outlined in the appendix.

PHYSICAL SLICE SELECTION NMR PROBES

In physical slice selection measurements the dimensions of the slice are controlled by the dimensions of the NMR coil and/or the position of any radiofrequency screening used. Two options exist; first a NMR probe whose length in the slice direction is comparable to the required slice dimension and, second, a longer NMR probe with the slice width being determined by radiofrequency screening. In this study physical slice selection probes based on these localization methods have been constructed and tested.

These probes are based on the "sine spaced" design of Bolinger *et al.*, (1988), which was selected on the basis of the required core sample and magnetic field orientation, low sensitivity to probe loading effects and ease of construction and frequency tuning. Schematic diagrams of the "short strut" and "radiofrequency screened" probes are presented in Figure 1. The axial (z) direction is parallel to that of the static magnetic field.

The dimensions of the short strut probe were selected to enable the detection of core porosity heterogeneities on a spatial scale of the order of 30mm. The copper NMR coil is 100mm in diameter and has 22, 10mm long struts. The coil is tuned to the NMR resonance frequency with four soldered chip capacitors (Morgan Matroc Type 101) and is inductively coupled to the transmitter output/receiver input. The NMR probe was constructed from low ^1H content materials in order to minimize the probe contribution to the ^1H NMR signal. Guard rings were installed in this probe to reduce the effect of magnetic and electric fields generated near the tuning capacitor elements. Since this NMR probe was built specifically to excite a small sample volume, the coil length to diameter ratio of 0.1 is less than optimal for producing a homogeneous B_1 field; usually it is desirable for this ratio to be greater than 1. The resulting spatial variation of B_1 is considered in the following sections.

The design of the radiofrequency screened probe is identical to that of the short strut probe in all respects except that the strut length of the former is increased to 160mm and a conductive copper mesh is used for radiofrequency screening of the sample. This probe was tuned to the NMR frequency by a combination of

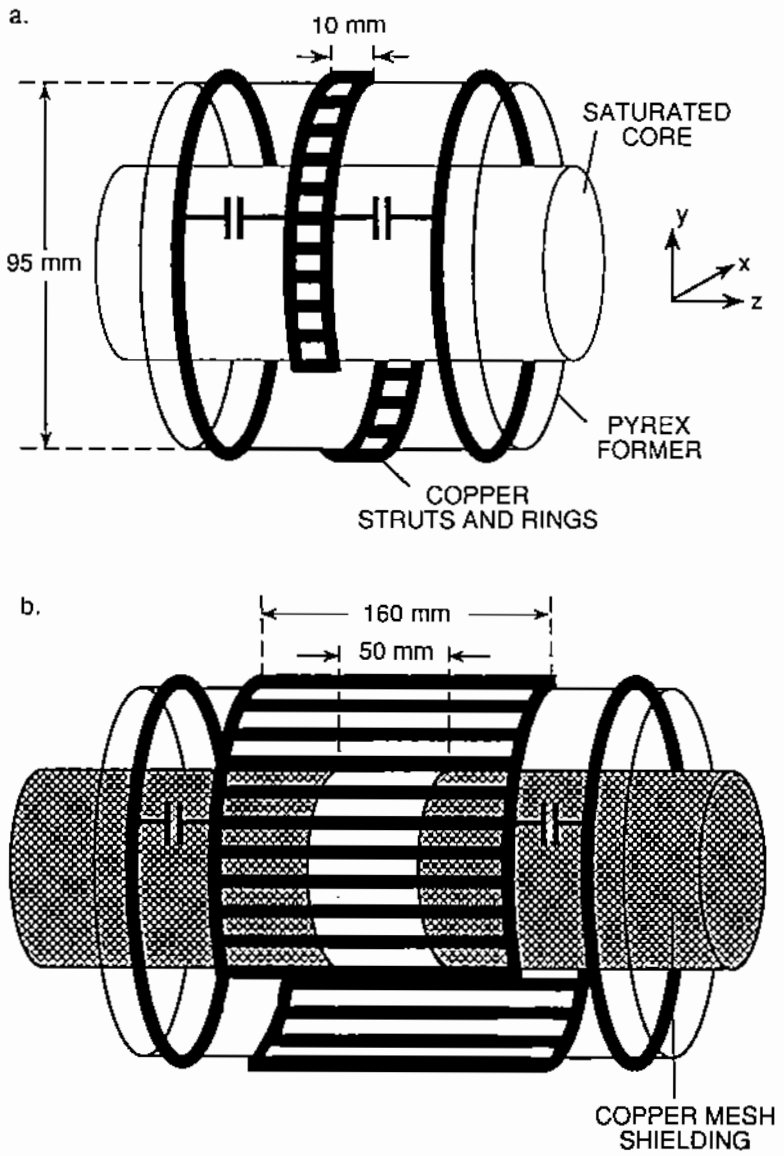

FIGURE 1 Schematic diagrams of (a) the short strut and (b) the radiofrequency-screened NMR probes.

four soldered chip capacitors and the position of the grounded copper mesh screens.

Axial Slice Definition of the NMR Probes

In order to correctly interpret data acquired with physical slice selection methods it is essential to know both the slice thickness and the variations in signal intensity across the defined slice. These can be ascertained from the slice profile of a reference sample obtained by Fourier transformation of a spin echo acquired in the presence of an applied magnetic field gradient (Lauterbur, 1973).

Axial (z) slice profiles obtained with a cylindrical water phantom (63mm diameter x 400mm length) are presented for the short strut probe as a function of pulse duration in Figure 2; the horizontal axis is directly proportional to distance since a linear field gradient was applied. A spin echo pulse sequence, t_p-delay-$2t_p$-delay-acquire, was used with pulse durations, t_p , of 40, 45, 50, 55 and 60 μs. The effective π/2 pulse was set to be 50 μs in duration. The changes observed in the slice profile as the pulse duration is varied arise from B_1 inhomogeneities within the probe; the magnitude of the B_1 magnetic field is greatest in the central region of the z-slice.

For z-axis spatial calibration purposes a slice profile of a water phantom (63mm diameter x 10mm length) was obtained with a 50 μs duration effective π/2 pulse. Defining the slice thickness as the profile width at half amplitude the slice thickness for the solid curve in Figure 2 is 30mm.

An equivalent axial (z) slice profile for the radiofrequency screened probe is presented in Figure 3. The "shoulders" observed are due to the presence of the conducting copper screens, placed 50mm apart, which distort the B_1 magnetic field. This slice profile could be altered by repositioning the copper screens.

Although either of the localization methods could be used to measure porosity profiles, the short strut probe was selected for all subsequent experiments.

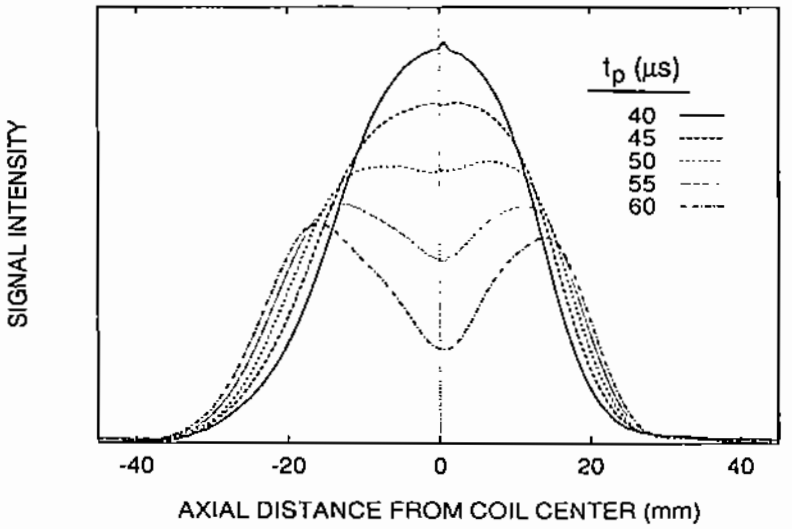

FIGURE 2. Short strut probe axial slice profiles for various pulse durations.

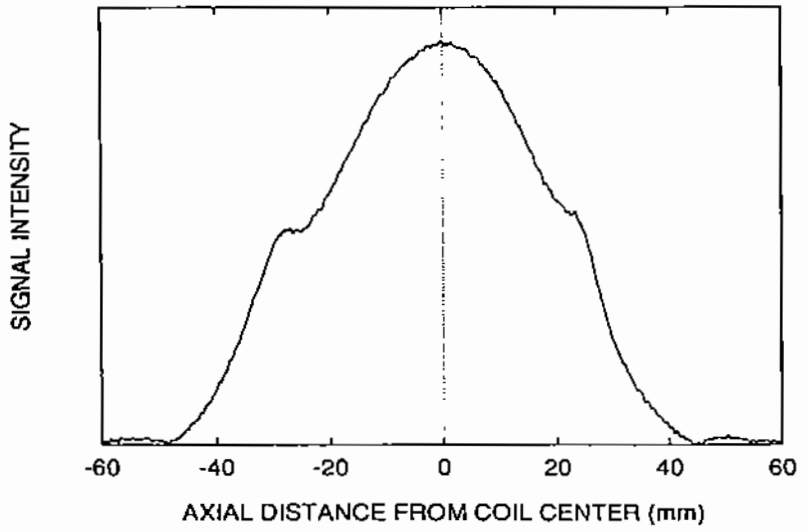

FIGURE 3. Axial slice profile obtained with the radiofrequency-screened probe.

B_1 Field Map of the Short Strut NMR Probe

Having obtained the slice profile for the short strut probe detailed B_1 maps (Murphy-Boesch *et al.*, 1987) were acquired for two slice orientations. Ideally, the B_1 field should be uniform in the transverse (xy) plane and sharply defined along the longitudinal (z) axis. However, the reality, using physical slice selection methods, is the variation in the B_1 field shown in Figures 4 and 5. This information is important to validate assumptions made in deriving the NMR protocol described later.

The B_1 map through the xy-plane perpendicular to the slice direction (z) is presented in Figure 4 in which the pixel intensity is directly proportional to the magnitude of the local B_1 field. The cylindrical slice phantom used in these experiments has a diameter of 63mm and a length of 10mm; the image is not circular due to the presence of an air bubble in the phantom. This image can be calibrated since the effective $\pi/2$ pulse was set to be 50 μs, which corresponds to a B_1 field of 1.2G; thus the B_1 field generated by the probe across the slice phantom varies from 2.4G at the bottom edge to 1.2G at the centre of the phantom. The B_1 field ranges from 1.2 to 1.8G across a 50mm diameter sample; this diameter excludes the dark band near the bottom edge of Figure 4, the origin of which is not yet understood.

The B_1 map through the yz-plane is presented in Figure 5; the absolute pixel intensities in this image are different from those of the B_1 map of the transverse slice due to image intensity scaling. Calculation of the B_1 values for the longitudinal slice by the method described above gives results which are consistent with those obtained for the transverse slice.

If no B_1 magnetic field variations were observed, then a water sample of any dimension could be used as a mass reference for porosity measurements. However, the variations in the B_1 field can be normalized by comparing the experimental data obtained from the core samples with that from a reference sample of the same diameter as the core, as shown in the following section.

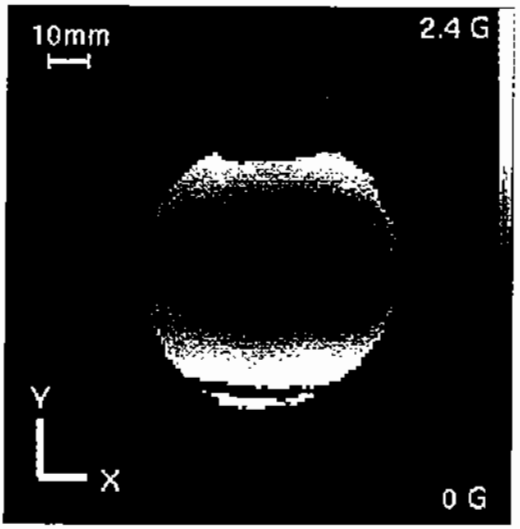

FIGURE 4. Transverse (xy) slice B_1 field map of the short strut probe. B_1 in gauss (G).

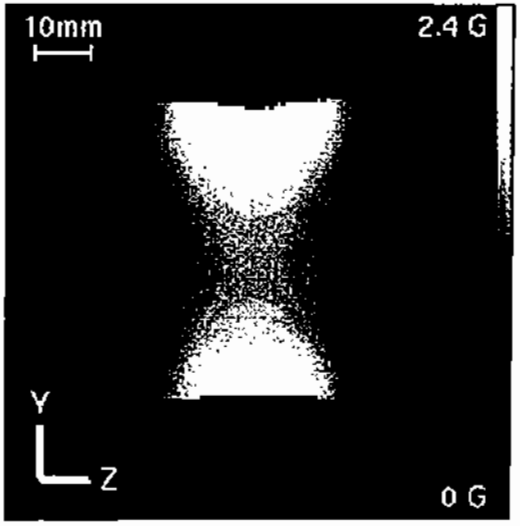

FIGURE 5. Longitudinal (yz) slice B_1 field map of the short strut probe. B_1 in gauss (G).

NMR PROTOCOL

In order to develop a robust NMR protocol for the accurate measurement of porosity in single-phase brine-saturated cores, we selected the simplest conceivable NMR experiment, namely the pulse-acquire sequence, Figure 6.

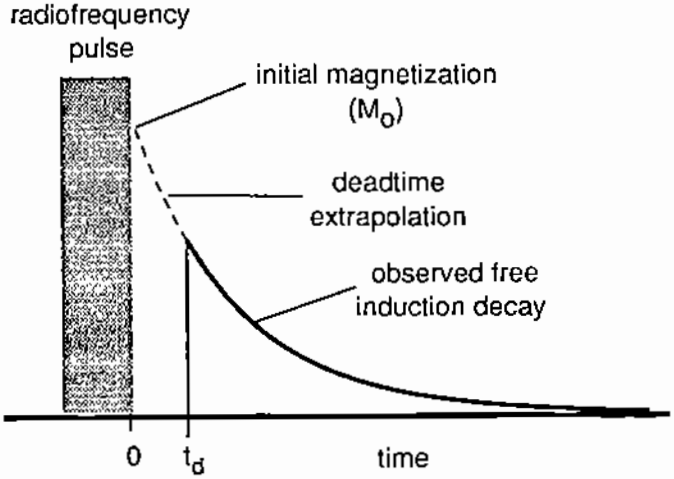

FIGURE 6. NMR pulse-acquire sequence used for the porosity measurements showing the deadtime (t_d) extrapolation.

In this sequence a single radiofrequency pulse is applied and the decaying NMR signal is sampled after the receiver deadtime. The signal amplitude immediately after the pulse is directly proportional to the sample magnetization, M_0, when appropriate NMR hardware and experimental parameters are selected; the latter are tabulated in Table 1.

TABLE 1. NMR Experimental Parameters.

Pulse duration	25μs
Receiver deadtime	25μs
Digitizer dwell time	1μs
Time domain points acquired	2048
Recycle time	7s
Number of scans	64

The pulse duration, 25 μs, corresponds to an effective $\pi/4$ pulse. The fastest digitizer rate available was employed to characterize the rapidly decaying time domain signals. The receiver deadtime prohibits acquisition of the important initial portion of the NMR signal. To obtain accurate M_0 values the data were processed to subtract contributions to the NMR signal arising from the probe and core wrapping materials. No correction for any residual NMR signal from the "dry" core was made.

A time domain data extrapolation method is required to account for signal loss during the receiver deadtime (see Figure 6). The magnitude data derived from the first 100 time domain points detected in quadrature, were fitted, using a nonlinear least squares fitting routine, to a stretched exponential function (Kenyon *et al.*, 1986; Lucas *et al.*) given by Equation (1).

$$M_{xy}(t) = M_0 \exp\left[-\left(t/T_2^*\right)^{\alpha}\right] \qquad (1)$$

In this expression the time (t) decay of the observed magnetization (M_{xy}) is described by an initial magnetization value (M_0), a time constant (T_2^*) and an exponent (α). This functional form accurately describes the observed multiexponential decay.

For bulk water in a homogeneous static magnetic field the time domain signal is a single exponential decay, producing a Lorentzian lineshape in the frequency domain. A normal distribution of local magnetic fields produces a superposition of Lorentzian lines yielding a Gaussian lineshape. The "stretched exponential" form represents both Lorentzian, Gaussian and mixed lineshapes depending on the value of the stretching exponent, α. The situation in core samples represents a mixture of these extremes (Lukyanov *et al.*, 1983). All the core samples studied are characterized with this simple function.

In order to convert the experimental NMR signal amplitudes into porosity values the NMR signal from a cylindrical glass vessel (400mm length x 50mm diameter) containing an aqueous 2.5mM $MnCl_2$ solution was used as a mass reference. The porosity was calculated using the following expression, derived from: (i) the fact

that the amplitude of the NMR signal is directly proportional to the ^1H content of the selected slice, (ii) the assumption that the pore fluid is homogeneously distributed across each transverse slice and (iii) the assumption that B_1 variations are insignificant over small radial distances.

$$\phi^{core} = \phi^{ref} \frac{M_0^{core} \rho^{ref} \chi^{ref} V_s^{ref}}{M_0^{ref} \rho^{core} \chi^{core} V_s^{core}} \qquad (2)$$

where ϕ is the porosity, M_0 is the magnetization, ρ is the fluid density, χ is the mass fraction of water in the fluid, V_s is the sample volume within the slice and the labels "core" and "ref" refer to the core and reference samples, respectively.

In principle the volume of the sample within the selected slice can be derived from the B_1 map; thus a porosity could be calculated directly. In practise assumption (ii) facilitates the use of a reference sample to calculate the porosity, normalizing the effect of B_1 inhomogeneities. The factor V_s^{ref}/V_s^{core} is replaced by $(D^{ref}/D^{core})^2$, where D is the sample diameter, since the axial slice thickness is constant. Assumption (iii) above requires that the diameters of the core and reference be nearly equal.

The fact that the recycle time between scans of 7s is greater than five times the longest spin lattice relaxation time component observed in these cores is inherent in the validity of Equation (2).

There are two additional factors affecting the applicability of Equation (2), namely (i) uniform pulse excitation and (ii) probe loading. The first arises from the differing NMR time domain signal decay rates (*i.e.*,NMR linewidths) observed for the core and reference samples. This is particularly important for the core samples with decay rates determined by the distribution of local magnetic fields imposed by susceptibility differences between the pore fluid and the rock matrix. The NMR linewidths for samples A, B, C, D and E, based upon a full width, half height criterion, are 180, 220, 700, 170 and 160Hz, respectively. The linewidths for the long Berea and Bedford samples are 680 and 160Hz. The effect of nonuniform excitation would result in the measured NMR porosity being systematically lower than the actual porosity. The second factor arises from a degradation in the NMR coil performance due to interaction between the coil and an electrically conducting

sample. Higher porosity cores are most susceptible to probe loading. The coil-to-core diameter ratio in these experiments (~2:1) was chosen to reduce such probe loading effects.

The NMR data were acquired at fixed spatial intervals, typically 10mm, along the length of the core sample; this interval was such that the selected slices overlapped, producing a smoothed profile.

CORE MEASUREMENTS

Physically slice selected NMR porosity profiles have been obtained for three long core samples. Two of these samples, Berea sandstone and Bedford limestone, are single cores of length greater than the slice thickness. The third sample is a composite constructed from five separate cores of different types, the length of each being comparable to the slice thickness.

Core Preparation

Descriptions of the seven core samples studied are given in Table 2. The core samples were cleaned by extraction with methanol in a Soxhlet apparatus for 48 h, air dried and vacuum dried at room temperature for a minimum of 48 h and weighed. The cores were placed under vacuum (≤1mbar) for 24 h then saturated with degassed brine (5.0 wt.% NaCl, 0.5 wt.% $CaCl_2$). The cores were stored in brine.

Prior to measurement excess brine was removed from the surface of the cores with a paper towel and the cores were wrapped in poly(vinyl chloride) film during measurements to reduce evaporation losses. The saturated mass of the cores was recorded before and after NMR measurements. The difference in these masses is negligible in comparison with the observed discrepancy between the water content measured by NMR and gravimetric methods.

TABLE 2. Core descriptions.

Sample	Description	D (mm)	L (mm)	Brine content (g)	Porosity (%)
-	Berea sandstone	50.8	205	57.33±0.05	13.4±0.1
-	Bedford limestone	51.2	349	98.3±0.2	13.3±0.1
A	Window Ledge carbonate	50.8	63.3	22.94±0.06	17.4±0.1
B	Sendji dolomite	50.6	63.5	40.06±0.02	30.5±0.2
C	Berea sandstone	50.3	63.0	26.53±0.08	20.6±0.2
D	Nubia C sandstone	48.6	57.2	11.65±0.06	10.7±0.1
E	Madison carbonate	48.6	63.3	28.64±0.06	23.7±0.2
-	Composite A-E	~50	~310	129.8±0.1	20.8±0.1

Berea Sandstone Porosity Profile

The gravimetric porosity of the long Berea sandstone core, with a mean diameter of 50.8mm and length 205mm, was 13.4±0.1%. The core was supported in the glass former of the NMR probe using Teflon rings. The core was moved through the probe in 10mm steps, the NMR porosity being determined at each position. The results were processed as previously described and the resulting porosity profile data are presented in Figure 7.

The results show the uniformity of the fluid distribution; the measured NMR porosity varied by less than one porosity unit across the sample. The low porosity values at the extremes in the profile are due to the core not completely filling the slice; these data should be disregarded. By integrating the NMR porosity profile numerically the mean NMR porosity for the sample can be computed and compared with the known value determined gravimetrically. The mean NMR porosity is 13.0±0.3%; the first and last three porosity values were omitted from this calculation. The

mean NMR porosity value is approximately 0.4% porosity units low compared with the gravimetric value. This underprediction by NMR is due to nonuniform excitation.

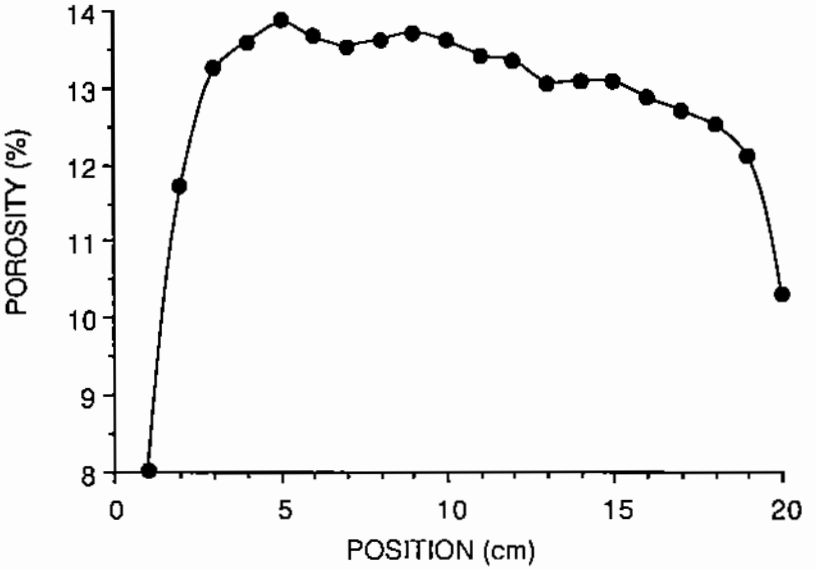

FIGURE 7. NMR porosity profile of the Berea sandstone core. Uncertainty of each point is approximately ±0.3-0.4% porosity.

Bedford Limestone Porosity Profile

The gravimetric porosity of the Bedford carbonate core, with a mean diameter of 51.2mm and length of 349mm, was 13.3±0.3%. This core was moved through the probe in 20mm steps with the NMR porosity being determined at each position. The results were processed as described previously and the resulting porosity profile data is presented in Figure 8.

Again a uniform fluid distribution is observed. The mean NMR porosity was calculated to be 13.8±0.3%, which is approximately

0.5% porosity high. Comparison with NMR brine saturation measurements for carbonate cores which fit completely within a NMR probe indicates that subtraction of the residual signal from the "dry" core will bring the result obtained here to within 0.2% porosity units of the gravimetric value. This correction would not be possible in an "on-line" NMR core analysis measurement.

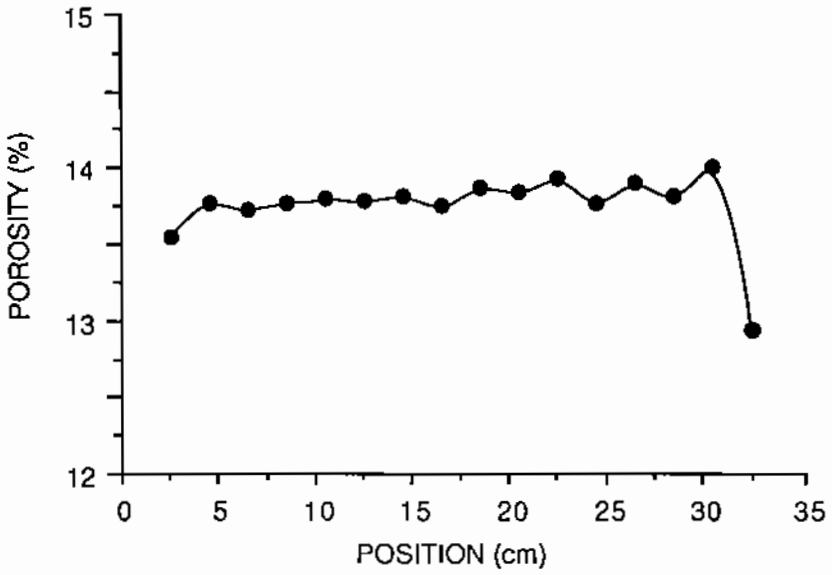

FIGURE 8. NMR porosity profile of the Bedford limestone core. Uncertainty of each point is approximately ±0.3-0.4% porosity.

Composite Sample Porosity Profile

The five cores, A, B, C, D and E, were assembled into a composite core to illustrate the spatial resolution attainable with the slice selection probe. The cores, detailed in Table 2, were arranged in sequence so that the porosity varied discontinuously along the sample. The composite core was moved through the probe in 10mm steps and data were acquired data at each position. The NMR and gravimetric porosity profile results are shown in Figure 9.

The NMR porosity profile clearly maps the trend in true porosity variation along the sample.

The effect of positioning the slice profile such that two cores are sampled simultaneously is clearly demonstrated by the smooth NMR porosity profile as compared with the known discontinuous gravimetric porosity profile. A minor complication is that each of the data points requires a separate volume correction due to core diameter variations. For the data presented here a simplified correction has been applied; the diameter of the core occupying the largest fraction of the slice was used in the calculation. However, when the slice is equally occupied by two cores, the mean of the core diameters was used.

A mean NMR porosity was calculated by numerically integrating the porosity profile and dividing by the integration range. This gives a value of 19.8±0.6% porosity; the gravimetric porosity was calculated similarly giving 20.8±0.1%. The first and last three points were excluded from these calculations due to incomplete filling of the slice. Thus, this result demonstrates the feasibility of spatially mapping heterogeneous brine saturations via this method.

Two actions can be considered to improve the accuracy of the results obtained for this composite core; either reduce the slice dimensions or incorporate software to deconvolve the NMR porosity profile with the known slice profile to produce a closer representation of the discontinuous gravimetric porosity. The first option is impractical since reducing the probe strut length will not reduce the slice thickness sufficiently and may even result in the probe not operating correctly, so the second approach is considered here.

The software developed was used to model our experiment by convolving the measured NMR axial slice profile with the discontinuous gravimetric porosity profile; the result is shown as the solid curve in Figure 9. This is the predicted NMR porosity profile. Comparison of the predicted curve with the experimental data demonstrates the good correspondence between the two, validating the assumptions inherent in Equation (2).

Preliminary investigation of the deconvolution of the measured NMR porosity profile with the NMR slice profile has been conducted and optimization of this technique is now in progress (Robson, 1991).

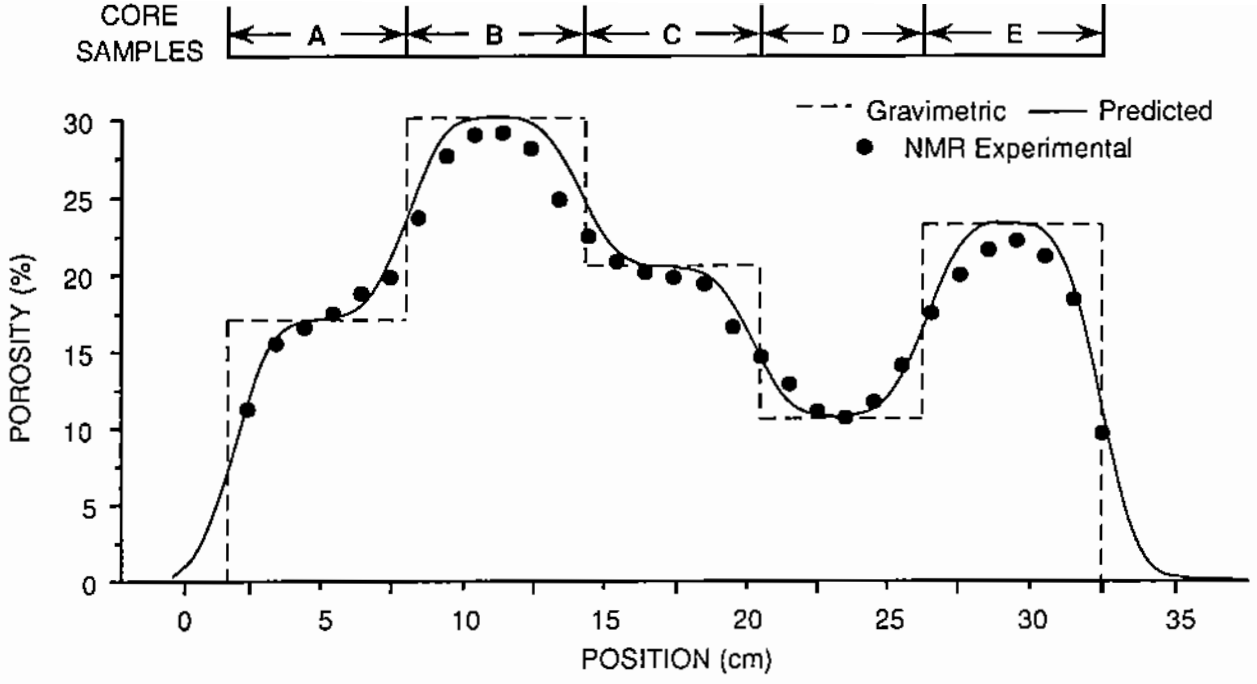

FIGURE 9. Comparison of porosity profiles for the composite core sample. Uncertainity of each NMR experimental point is approximately ± 0.6% porosity.

CONCLUSION

NMR coils have been tested and a protocol developed for the measurement of porosity profiles in long core samples by the use of physical slice selection. The feasibility of mapping porosity via this method was demonstrated with three brine-saturated long core samples: a Berea sandstone, a Bedford limestone and a composite sample consisting of five different short cores.

An important extension of this method is that porosity maps of mixed-phase saturated cores can readily be obtained using the approximation that ^1H densities in oil are equal to that in brine (0.11 mol/cm^{-3}).

The measurements reported here were based upon an acquisition time of 5-7 minutes per point on the porosity profile. By further optimizing the NMR parameters it is quite feasible to expect the total time for acquisition and data processing to be less than 1 minute per point.

To our knowledge these are the first published porosity profiles obtained with physically slice selected NMR. The close agreement between NMR and gravimetric data for these three cores demonstrates the accuracy and practicality of porosity mapping with this method. The physical slice selection technique described here is applicable to a much wider range of core samples than can be studied quantitatively with NMR imaging methods.

ACKNOWLEDGEMENTS

AJL, GKP and MP wish to thank Amoco (UK) Exploration Company for project support. LDH and TAC thank Dr Herchel Smith for his generous endowment. The authors wish to thank Matthew D. Robson for the convolution / deconvolution results and Clifford S. Bunch for technical assistance.

REFERENCES

BOLINGER, L., PRAMMER, M.G. and LEIGH, J.S.(1988). A multiple frequency coil with a highly uniform B_1 field. *Journal of Magnetic Resonance*, 81 (1),162-166

EDELSTEIN, W.A., VINEGAR, H.J., TUTUNJIAN, P.N., ROEMER, P.B. and MUELLER, O.M. (1988). NMR imaging for core analysis. In *Proceedings,of the 63rd Annual Technical Conference of the*

Society of Petroleum Engineers (Houston TX, October 1988), p. 101-112, SPE 18272

EDELSTEIN, W.A., VINEGAR, H.J., TUTUNJIAN, P.N. and ROEMER, P.B. (1990). Time domain curve fitting for automated oil core NMR spectral analysis. In *Proceedings of the 4th Annual Technical Conference of the Society of Core Analysts*, Paper 9025

GUILFOYLE, D.N., MANSFIELD, P. and PACKER, K.J. (1992) Fluid flow measurement in porous media by echo planar imaging. *Journal of Magnetic Resonance*, **97** (2), 342-358

KENYON, W.E., DAY, P.I., STRALEY, C. and WILLEMSEN, J.F. (1986) Compact and consistent representation of rock NMR data for permeability estimation. In *Proceedings of the 61th Annual Technical Conference of the Society of Petroleum Engineers* (New Orleans LA, October 1986)., p 1-22, SPE 15643

LAUTERBUR, P.C. (1973) Image formation by induced local interactions: examples employing nuclear magnetic resonance. *Nature*, **242**, 190-191

LUCAS, A.J., PIERENS, G.K., PEYRON, M., HALL, L.D., STEWART, R.C., POTTER, G.F. Quantitative determination of porosity in a variety of reservoir rock cores by NMR (in preparation)

LUKYANOV, A.E., BULYGIN, A.N. and NIKOLAEV, B.P. (1983) NMR lineshape calculation for a liquid in a porous medium. *Colloid Journal of the USSR*, **45** (1), 65-69

MITRA, P.P.and SEN, P.N. (1992) Effects of microgeometry and surface relaxation on NMR pulsed field gradient experiments: simple pore geometries. *Physical Reviews B* , **45** (1) 143-156

MURPHY-BOESCH, J., SO, G.J. and JAMES, T.L. (1987) Precision mapping of the B_1 field using the rotating frame experiment. *Journal of Magnetic Resonance*, **73** (2), 293-303

OSMENT, P.A., PACKER K.J., TAYLOR, M.J., ATTARD, J.J., CARPENTER T.A., HALL, L.D., HERROD, N.J. and DORAN S.J. (1990).NMR imaging of fluids in porous solids. *Philosophical Transactions of the Royal Society Series A*, **333** (1632), 441-452

ROBSON, M.D.(1991) Image restoration in nuclear magnetic resonance imaging. University of Cambridge,(unpublished)

SANDERS, J.K.M. and HUNTER, B.K. (1987). *Modern NMR Spectroscopy.* Oxford: Oxford University Press

THOMAS, D.C. and PUGH, V.J. (1989) A statistical analysis of the accuracy and reproducibility of standard core analysis. *The Log Analyst*, March-April, 71-77

VINEGAR, H.J., TUTUNJIAN, P.N., EDELSTEIN, W.A. and ROEMER, P.B. (1989) ^{13}C NMR of whole cores. *Proceedings of the 64th Annual Technical Conference of the Society of Petroleum Engineers* (San Antonio, TX,October 1989), p 201-212. SPE 19590

WOESSNER, D.E., GLEESON, J.W. and JORDAN, C.F. (1990) NMR imaging of pore structures in limestones. *Proceedings of the 65th Annual Technical Conference of the Society of Petroleum Engineers* (New Orleans LA,September 1990), p.19-25. SPE 20493

APPENDIX

NMR is a technique (Lauterbur, 1973, Sanders and Hunter, 1987) that exploits the fact that certain nuclei, in our case ^1H, possess spin, I, with an associated magnetic moment, μ, which is able to interact with an applied static magnetic field, B_0. This interaction produces a macroscopic magnetization, M_0, which is parallel with B_0 and directly proportional to the number of ^1H nuclei in the sample. The magnetization, M_0, is rotated away from the direction of B_0 by applying a pulsed magnetic field B_1 perpendicular to B_0 and rotating at the NMR resonance frequency, ω, given by

$$\omega = \gamma B_0 \qquad \text{(A1)}$$

where γ is the magnetogyric ratio. M_0 is rotated through an angle θ where

$$\theta = \gamma B_1 t_p \qquad \text{(A2)}$$

and t_p is the time for which B_1 is applied. Following the B_1 pulse the magnetization precesses about B_0 at the NMR resonance frequency. This induces a current in the NMR coil which is

detected as the NMR signal. The amplitude of this signal is proportional to $M_0\sin(\gamma B_1 t_p)$, the component of M_0 perpendicular to B_0.

In a homogeneous magnetic field the relaxation of magnetization toward equilibrium is characterized by the spin-lattice relaxation time, T_1, for components parallel to B_0 and the spin-spin relaxation time ,T_2, for components perpendicular to B_0. Due to the presence of magnetic field inhomogeneities the individual spins precess at different rates and the phase coherence producing the resultant magnetization is lost. The decay of the NMR signal is then characterized by T_2^*.

Phase coherence can be restored by applying a second B_1 pulse. The resulting NMR signal is termed a spin echo.

Spatial information can be obtained by making the applied magnetic field a function of position, **r**, within the sample, using magnetic field gradients, **G** (Lauterbur, 1973). The NMR resonance frequency is then

$$\omega = \gamma(B_0 + \mathbf{r}.\mathbf{G}) \qquad \text{(A3)}$$

The resonance frequencies can be extracted from the NMR signal by Fourier transformation of the NMR signal.